Numerical and experimental study of the steady-state radial heat conduction

Javier Cardenas Gutierrez
Engineering Faculty
Universidad Francisco de Paula Santander, Cúcuta, Norte de Santander, Colombia
Email- javieralfonsocg@ufps.edu.co

Jhan Piero Rojas
Engineering Faculty
Universidad Francisco de Paula Santander, Cúcuta, Norte de Santander, Colombia
Email- jhanpierorojas@ufps.edu.co

Gonzalo Romero Garcia
Engineering Faculty
Universidad Francisco de Paula Santander, Cúcuta, Norte de Santander, Colombia
Email- gonzalodelacruzrg@ufps.edu.co

Abstract- There is proposed the experimental determination of the coefficient of thermal conductivity for different from materials by means of a team of measurement of heat transfer in radial form, which consists of a central resistance which leads heat to a metallic disc with a central hole, for the information reception one is provided with a series of uniformly distant sensors of temperature which are placed in form perpendicular to the surface of the disc of tests, an Arduino® connected to a computer takes these signs and prints the values of temperature of every sensor on a table of Excel, there the information is organized, tabulated and charted. From a simulation using a software CAD (Solidworks ®), could visualize the temperature profile for every material. Using a mathematical algorithm in Excel the coefficient of thermal conductivity proceeds to be from the information tabulated previously, these values are charted and compared along with obtained theoretical values of the specializing stage of heat transfer in order to determine the percentage of error of the obtained values of the coefficient of thermal conductivity of experimental form.

Keywords – Educational tool, learning, radial heat transfer, coefficient of thermal conductivity.

I. INTRODUCTION

Heat transfer is a basic applied engineering science, which is included in the curricula in many of its branches, such as Mechanical Engineering and Chemical Engineering [1],[2]. The students who take this course need to develop a solid knowledge, both theoretical and practical, of this science since in the industry it is common to relate to processes related to heat conduction, among which are the heat treatments carried out on steels, the use of steel and its alloys on the design of heat exchangers for heat dissipation [3], heat conduction in machined materials due to high cutting speeds [4],[5], It should be noted that according to Lookman and Bel [6] the losses in an electric motor amount to a value of between 4 and 24% of its nominal power, this power lost being converted into heat and transferred to the environment.

In order to evidence the heat transfer mode mentioned above, it is proposed to implement a radial heat conduction unit with the purpose of validating the basic concepts of heat conduction such as thermal conductivity, the effect of this on temperature distribution, the elaboration of temperature profiles in different types of materials; besides that, the obtaining of data that can later be processed by means of software for the analysis of the error among the results. Among the commercial solutions are the ones proposed by Kern [7], who presents a piece of equipment for the determination of the thermal conductivity of non-metallic solids, consisting of an electric heating plate, two identical test specimens through which the heat flows and two water jackets used to remove the heat, and by means of thermocouples the temperature in both phases of the specimen is measured.

Edibon [8] develops the computer-controlled heat conduction unit, which is provided with a metal disk for performing a series of radial heat conduction experiments. The unit is supplied with interchangeable samples of different materials,

diameters, and insulating materials, which make it possible to demonstrate the effects of area, conductivity, and series combinations on heat transfer processes. Méndez Lango et al. [9] use the primary method used at the National Center of Metrology (CENAM) for measuring the thermal conductivity of insulating solids: a hot plate device with guard (APCG). They present a model to study heat transfer in the annular space of a hot plate, which can be used to estimate the magnitude of heat flow under different operating conditions between the measurement area and the hot plate guard. The results show that the main contribution to the heat flow in the annular space is the heat conduction in the air through the annular space, and the other effects can be considered negligible for all practical purposes.

Lira Cortés et al.[10] implement a thermal conductivity measurement system for solid conductive materials by developing the design criteria for the construction of the measurement system, which operates under a steady-state heat flow condition using a reference material, which limits its operating range by its conductivity value and geometric dimensions. M. A. Ventura[11] develops two models (one stationary and one transient) to simulate radial driving in a fuel element and element sleeve. It adopts the hypothesis of the representation of concentrated parameters; these models are verified and compared with other similar ones. Included in the stationary model is a method for calculating the conductance of the gap between the UO_2 pellet and the fuel assembly sleeve and the uncertainty associated with its value.

W. Q. Li et al.[12] designed an experimental apparatus to measure the effective thermal conductivity of porous stainless steel fiber felt under different operating pressures. The total effective thermal conductivity was studied by analyzing the heat conduction of the matrix, the natural air convection, and the thermal radiation of the matrix at ambient pressure. The contribution of natural air convection was obtained experimentally by changing the ambient pressure under vacuum condition, and the solid matrix heat conduction was evaluated using a theoretical model. Palacios Alquisira [13] presents a laboratory work in which students must infer the concept of thermal conductivity of a material for its application in a real situation that requires the selection of the material for the design of a reactor. Y.Z. Povstenko[14] performs an investigation where the theory of thermal stresses based on the heat conduction equation with the time-fractional derivative of Caputo de orden α is used to investigate thermal stresses in an infinite body with a circular cylindrical hole. The solution is obtained by applying integral Laplace, and Weber transforms. Several examples of problems with Dirichlet and Neumann boundary conditions are presented, and the numerical results are illustrated graphically.

Buttsworth et al.[15] expresses that convective heat transfer data is often obtained from transient surface temperature measurements. Thin-film resistance calibrators, thermocouples, and thermochromic liquid crystals are used in various situations to measure surface temperature. Assuming uniform conditions of semi-infinite flat plates, it is possible to express instantaneous surface heat flow as an analytical function of transient surface temperature. Various approaches can be used to explain the presence of multilayer substrates and finite thickness substrate effects (Schultz and Jones, Doorly and Oldfield, Guo et al.). However, the effects of surface curvature are generally neglected.

Aaron J. Schmidt et al. [16] explore the relationship between impulse build-up and radial heat conduction in the transient resistance of the pump probe (TTR). The results illustrate how the accumulation of pulses allows TTR to simultaneously run two thermal length scales. Furthermore, the conditions under which the effects of radial transport are important are described; an analytical solution for anisotropic heat flow in stratified structures and a method for measuring the inter-plane and in-plane thermal conductivities of thermally anisotropic thin films are described. As a verification, the technique is used to extract the cross-plane and thermal conductivities in the plane of highly ordered pyrolytic graphite.

In this work, a theoretical-numeric-experimental comparison was made between the temperatures of a radial heat conduction unit heated by means of electrical resistance, whose results are compared with the heat conduction equation for a cylinder developed for the specific case. Likewise, the results achieved are verified with the use of a CAD type software that supports heat transfer simulations (SolidWorks ®).

II. Methodology

The following sections describe in detail the analytical and descriptive reasoning of the equipment for conducting the experimental study.

2.1 Theoretical analysis –

Starting from the unidimensional heat conduction through a cylinder, shown in Figure 1, a differential element is taken, which can be seen in Figure 2, and an energy balance is made, resulting in equation (1).

$$E_{in} + E_g = E_{out} + E_{ss}. \tag{1}$$

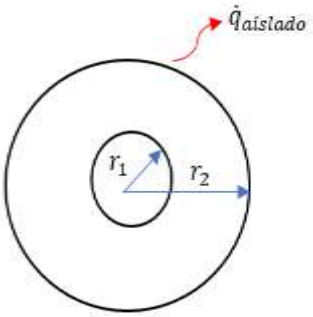

Figure 1. One-dimensional heat conduction through a cylinder.

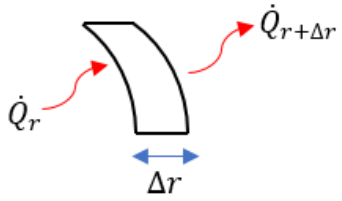

Figure 2. Differential element removed from the cylinder.

Taking into account that there is no power generation, that the power transfer is stationary and that the only power transfer is by heat, there is the equation (2)

$$\frac{d}{dr}\left[\dot{Q}_{(r)}\right] = 0 \tag{2}$$

where $Q(\dot{r}) = -kA\frac{dT}{dr}$, since the heat transfer is by conduction and A is the area of the cylinder given by $A = 2\pi rL$, is replaced in equation (3), and integrating both sides, that get

$$\frac{d}{dr}\left[-k2\pi rL\frac{dT}{dr}\right] = 0$$

$$T_{(r)} = C_1 \ln\frac{r}{r_1} + T_1 + C_2 \tag{3}$$

where $T_{(r)}$ is the temperature distribution. For this particular case, $r_2 = T_2$ and $r_1 = T_1$,

$$C_2 = \frac{(T_2 - T_1)\ln(1)}{\ln\frac{r_2}{r_1} + \ln(1)} \tag{4}$$

$$C_1 = \frac{T_2 - T_1}{\ln\frac{r_2}{r_1} + \ln(1)} \tag{5}$$

When the constants C_1 and C_2, equation (4) and (5), are found, these values are replaced in equation (6)

$$T_{(r)} = \left[\frac{T_2 - T_1}{\ln\frac{r_2}{r_1} + \ln(1)}\right]\ln\frac{r}{r_1} + T_1 + \frac{(T_2 - T_1)}{\frac{\ln {}^{r_2}/_{r_1}}{\ln(1)} + 1} \quad (6)$$

Equation (6) is finally the temperature of the cylinder as a function of its radius. The equation shown is then taken again to find the heat conducted through the cylinder.

$$r\frac{dT}{dr} = C_1$$

$$\frac{dT}{dr} = \frac{C_1}{r} \quad (7)$$

Equation (5) is replaced by equation (8)

$$\frac{dT}{dr} = \frac{\frac{T_2 - T_1}{\ln\frac{r_2}{r_1} + \ln(1)}}{r} \quad (8)$$

It is also known that the heat conduction equation is $\dot{Q} = -kA\frac{dT}{dr}$,, therefore $\frac{dT}{dr}$ is removed from the above expression and replaced in equation (9), is the one that models the heat conduction for the case study carried out.

$$\dot{Q} = -k2\pi L\left[\frac{T_2 - T_1}{\ln\frac{r_2}{r_1} + \ln(1)}\right] \quad (9)$$

2.2. Specifications of the heat conduction unit –

The radial heat conduction unit shown in Figure 3 has been built by the team to carry out the readings of the different temperatures along the radius of the cylinder (disc), which will later be compared with the theoretical analysis and the respective simulations.

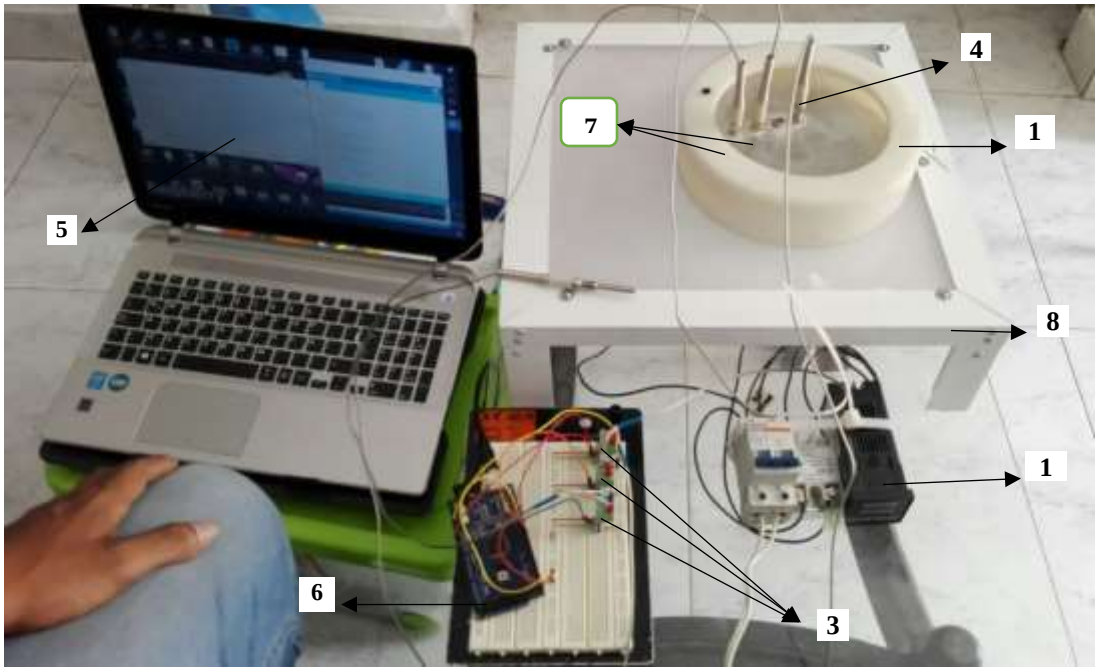

Figure 3. Schematic diagram of the refrigeration cycle (SRC).

The equipment has a heating unit composed of a thermoelectric resistor (3) and a PID control device (2). The temperature is manually graduated in the controller by means of a thermal sensor (4) that controls the temperature of the resistor by cutting or opening the electrical flow to the resistor as necessary to maintain the temperature at the previously set value, The test discs have an external diameter of 19.9 cm and an internal diameter of 13 mm, in which the resistance is fixed by means of an adjustment, each disc has a coating on its backside of a thermal insulator in foam, which prevents or minimizes heat loss in the longitudinal direction of the disc, in addition, small blind holes were drilled in the radial direction, spaced 2 cm which will serve as a seat for the thermal sensors. A 20cm internal diameter, 5mm thick, and 10cm high cylindrical hollow casing (1) isolate the system from the environment. This casing is crowned with a transparent acrylic disc drilled with holes where the three thermal sensors (7) that come into contact with the plates are inserted, The signals emitted by these sensors reach small MAXX6675 modules which condition the signal to be read by an ARDUINO MEGA (6), this processes the data and prints it on a computer screen (5) where the data is recorded and tabulated. The disks are interchangeable elements, one is made of aluminum, and the other is made of carbon steel ASTM A36. The whole system is supported on a structure made of rectangular aluminum profiles (8) that supports an acrylic sheet of 5mm thickness and 900cm square area.

When a value is assigned for the temperature at which the disk is to be heated, a certain time must have waited for it to reach a stable state and then, the temperatures recorded by the three thermocouples located along the radius of the disk are taken. As input temperatures are taken 65°C, 70°C, 75°C, 80°C and 85°C and, from them, five different temperatures are taken through the thermocouples. Table 1 below summarizes the characteristics of the radial heat conduction unit.

Table 1. Characteristics of the radial heat conduction unit.

Resistance diameter	12.90 mm
Power supplied by the resistor	50 W
Aluminum disc diameter	196.48 mm
Carbon steel disc diameter ASTM A36	198.65 mm
Number of thermocouples	4
Distance between thermocouples	2 cm
Thermal conductivity of aluminum	209.3 W/mK
Thermal conductivity stainless steel 304	16.3W/mK
Thermal conductivity carbon steel ASTM A36	59 W/mK
Insulating material discs	Polyurethane foam

2.3. Experimental analysis –

For this work, data was taken from two test discs, one of aluminum with a diameter of 196.48 mm and the other of carbon steel ASTM A36 with a diameter of 198.65 mm. The experimental procedure begins when the disc is placed in its place, in contact with the thermal resistance; after thermally sealing the device with the nylon casing, the three thermocouples are adjusted in their positions bypassing the upper acrylic sheet through their holes until they come into contact with the holes drilled in the test disc, After waiting 15 minutes while the equilibrium or stationary state is reached, we start with the data capture from an initial temperature of 65ºC, varying the temperature by 5ºC for each run until reaching 90ºC, for each one of these temperatures we take ten temperatures for each position, with the objective of obtaining a reliable average value for each temperature, then, each one of these data was organized, tabulated and graphed in Excel® for better visualization of the temperature behavior with respect to the position of each temperature sensor.

III. RESULTS AND DISCUSSION

3.1. Experimental results –

The average data of the temperature of each run for each material is tabulated and graphed below, in Table 2. The data of temperature of carbon steel ASTM A36, for 5 runs, from an initial temperature of 65ºC, being varied in 5 degrees for each run, until 85ºC, being compared with the temperature provided by the thermal sensors located at a distance of 2.4 and 6 cm of radial distance.

Table 2. Experimental sensor data taken for the steel disc.

	PID Therm. Sensor (0cm)	Thermocouple 1 (2cm)	Thermocouple 2 (2cm)	Thermocouple 3 (2cm)
Temperature 1	65	43.82	40.54	35.32
Temperature 2	70	44.27	41.37	39.72
Temperature 3	75	45.45	42.9	41.77
Temperature 4	80	48.27	45.12	42.42
Temperature 5	85	55.42	49.72	46.4

In Figure 4 is observed the form as the temperature begins to diminish as we move away of the center of the disk, where the flow of heat is conducted from the thermal unit, this diminution is not linear, as of the point 4, the diminution of the temperature is reduced, and its behavior tends to a constant line, this means, that as we approach the circumference of the disk, the temperature stops being affected significantly by the increase of the flow of heat yielded by the thermal unit, is this a direct effect of its thermal conductivity.

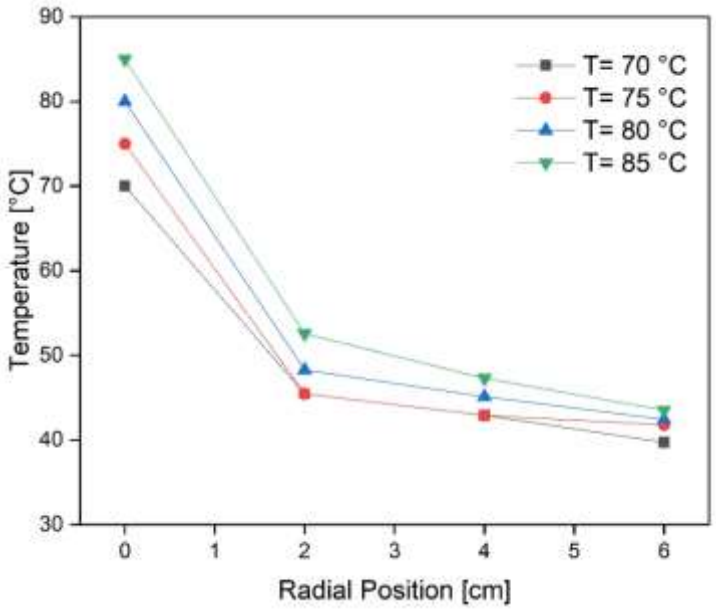

Figure 4. Temperature profile of Steel A36.

In Table 3 are tabulated the average temperature data for aluminum, as for carbon steel, 5 runs were made and the operating temperatures are compared with the temperatures obtained by the thermal sensors that are arranged at 2, 4 and 6 Cm from the center of the disk.

Table 3. Experimental sensor data taken for the aluminum disc.

	PID Therm. Sensor (0cm)	Thermocouple 1 (2cm)	Thermocouple 2 (2cm)	Thermocouple 3 (2cm)
Temperature 1	65	45.43	46.03	46.38
Temperature 2	70	47.20	41.00	48.03
Temperature 3	75	48.55	49.38	49.93

Temperature 4	80	50.75	51.28	51.13
Temperature 5	85	51.25	51.39	51.56

In Figure 5 are tabulated experimental data from Table 3. Thermal data is shown for the aluminum disc and can see how the heat is distributed in the disc in the radial direction, forming a characteristic temperature profile, although it follows a slightly similar behavior as the steel, you can see that the difference between initial and final temperature is not as high as in the case of steel, the behavior of these curves is compared with previous test disc, softer, this means that the heat presents less resistance as it moves in the radial direction in the disc.

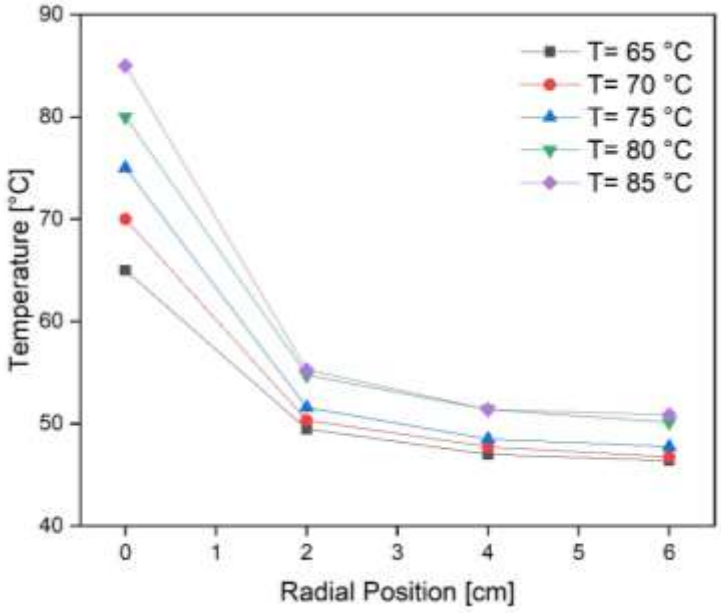

Figure 5. Temperature profile of aluminium.

3.2. Simulation –

The results of the simulation are presented in the graphs corresponding to the experiment with the help of Solidworks®, selecting the material Steel for this case. In Figure 6, it is shown how the points where the thermocouples are located on the disk, where an expected maximum temperature is reflected in the center of the circle, in which the temperature sensor is located (Point 1).

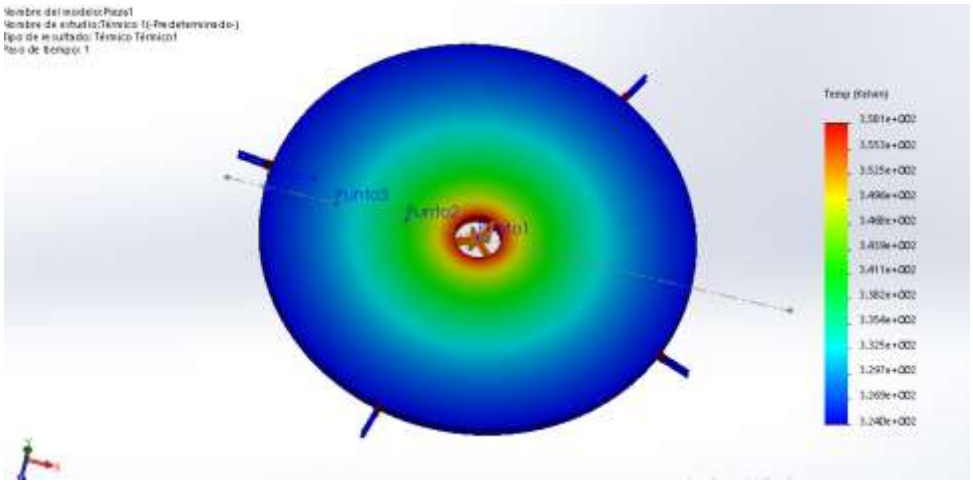

Figure 6. Steel Disc Simulation in Solidworks.

With this, the temperature profile of the simulated steel disk is made for the five corresponding temperatures, which can be seen in Figure 7. A descending behavior is observed, according to the results expected in the literature, in which, after 4 cm, the space between each of the points decreases, and they take values for when they reach 6 cm of 35.33, 46, 46.38, 50.13 and 51.35 respectively.

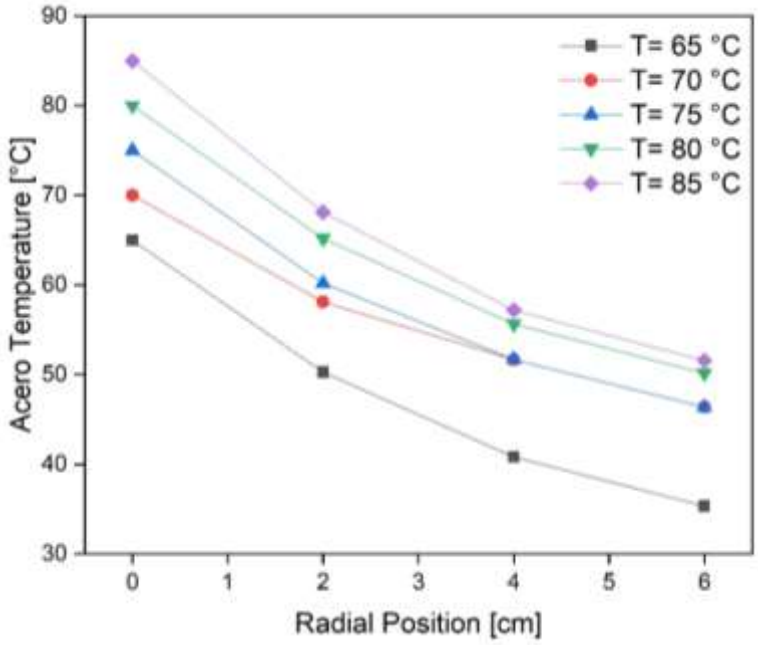

Figure 7. Temperature profile of simulated steel at Solidworks.

On the other hand, the simulation of the disk is carried out, taking the same points as in the previous simulation, but in this case, aluminum will be used as the material. The results of the simulation are shown in Figure 8.

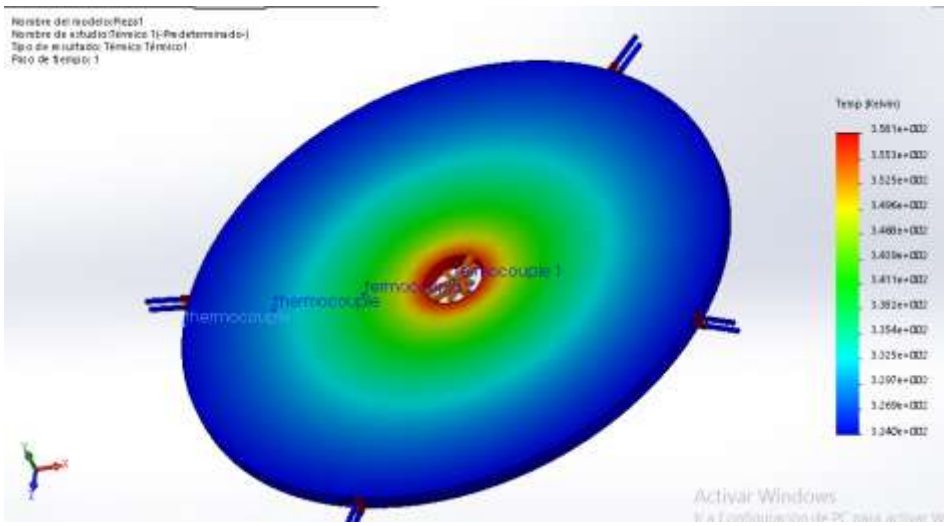

Figure 8. Aluminium Disc Simulation in Solidworks.

In Figure 9, the temperature profile shown in the simulation in Figure # is carried out. It shows a behavior as expected as heatwaves react. However, compared to the behavior obtained by the simulation with the material Steel, it is more compact, and the same behavior is seen in all the temperatures where it is analyzed.

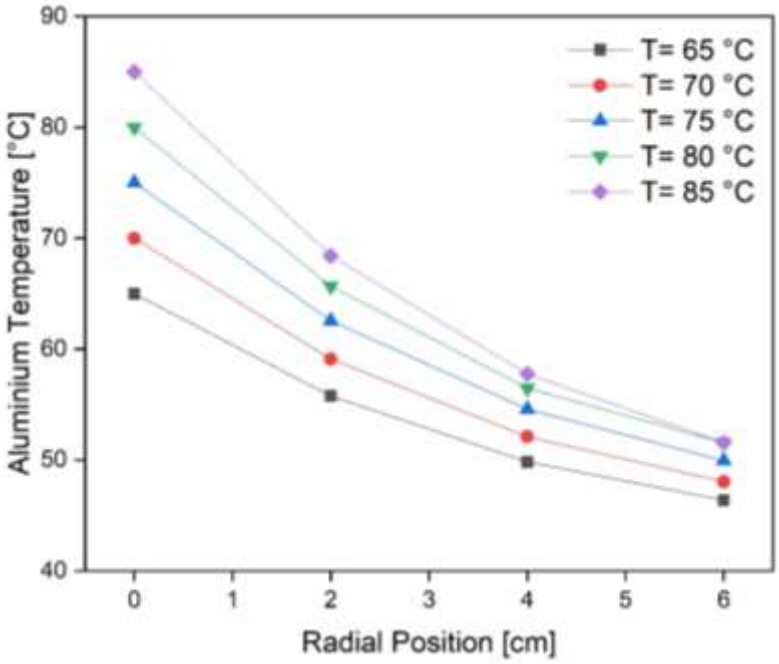

Figure 9. Temperature profile of simulated aluminium at Solidworks.

Figure 10 shows the comparison between the experimental tests and simulations for the temperatures 65 °C, 70 °C and 75 °C using aluminum as a material. A line behavior is shown for the experimental ones, reaching for the three temperatures 46.38°C, 48.03°C, and 49.93°C respectively. The results with respect to the simulation show an approximate reduction of 29% for the three from thermocouple 1, which is in the center of the disk, to thermocouple 2 located 2 centimeters from the center, while for the other thermocouples it does not exceed 1%.

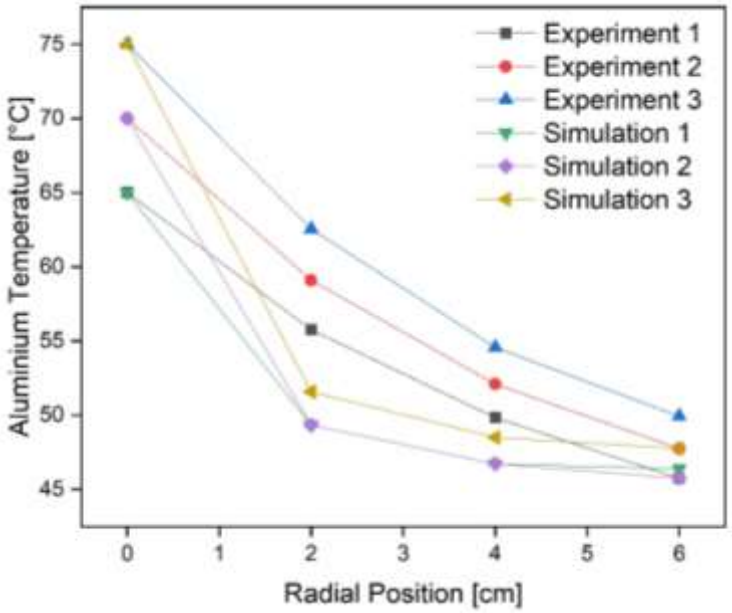

Figure 10. Experimental vs. simulated aluminum temperature profile in Solidworks.

As shown in Figure 11, experimental data is plotted at 65°C and 70°C and simulation data given by SolidWorks® at 65°C and 70°C using steel as the material. For the experimental data at 65 °C and 70 °C, an almost linear behavior is denoted for the temperatures taken by the thermocouples, having as centimeter six temperatures of 35.33 °C and 46 °C respectively. With respect to the experimental data, a curved behavior is denoted, which takes a linear behavior after the thermocouple is placed in the radial position at 4 centimeters. Its final thermocouple values vary from the experimental ones by 0 % and 13.63 %, respectively.

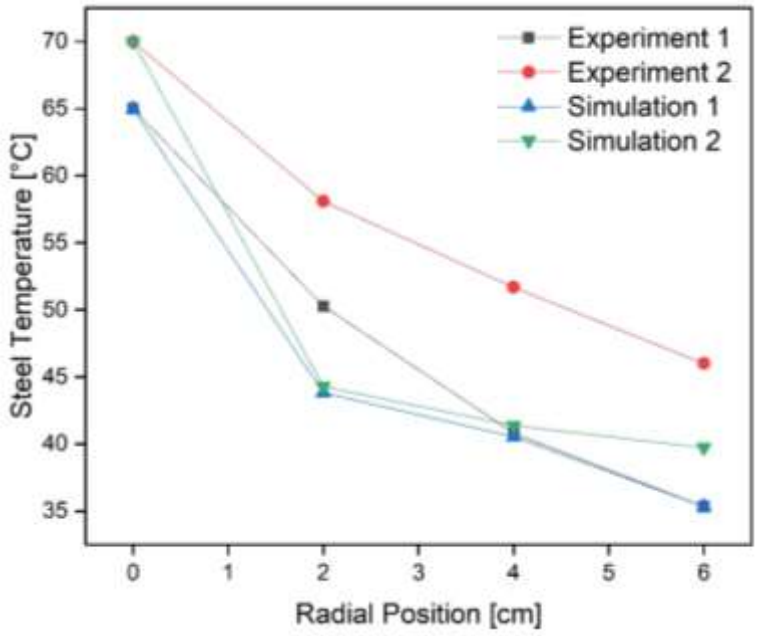

Figure 11. Temperature profile of simulated A36 steel at Solidworks.

IV.CONCLUSION

This article presents an experimental unit of radial heat conduction in a steady-state. The realization of this prototype generated a series of deliverables that allowed its realization, one of the first contributions has been the guide for the correct operation of the equipment and the necessary considerations to achieve the complete idealization of the process in addition to the present article which focuses the theoretical-simulated part of the heat-conducting unit.
The final result is the temperature profiles of the two types of metals used in the process, which allows us to corroborate the radial thermal conductivity of the analyzed materials in a practical, analytical and simulated way.

It is possible to visualize in the temperature profiles of each one of the materials their behavior decreases as we move away from the center of the disk, this decrease is not a line for any of the metals, but it is possible to observe a line trend from the point 4 equivalent to the thermocouple number 3.

In addition, the influence of the initial temperature in the radial conduction is emphasized because between greater temperature, its percentage of heat transmitted with respect to the time diminishes considerably, this appears in the metals steel A36 and aluminum.

The design of the heat conducting unit in the SolidWorks software that includes the simulations by means of this software for the verification of the theoretical and practical results.

NOMENCLATURES AND SYMBOLS

A_S	Surface area, m^2
A_{paso}	Pass area, m^2
A_{total}	Total heat transfer area, m^2

C_P	Fluid heat capacity, $\frac{J}{Kg} - K$
C_{min}	Minimum capacitance, W/K
C_{max}	Maximum capacitance W/K
Cr	Ratio of thermal capacitances
D_{int}	Internal pipe diameter, m
D_{ext}	Outside pipe diameter, m
$D_{intcarc}$	Internal diameter of the housing, m
D_e	Equivalent diameter, m
ε	Effectiveness
f	Friction factor
G_s	Mass velocity, $kg/m^2 s$
h_i	Internal convective coefficient, $W/m^2 K$
h_o	External convective coefficient, $W/m^2 K$
k	Fluid thermal conductivity, $W/m \cdot K$
k_{mat}	Material termal conductivity, $W/m \cdot K$
L_{carc}	Housing length, m
L_t	Pipe length, m
m_{carc}	Mass flow within the housing, kg/s
m_{carc}	Mass flow within the tubes, kg/s
N_b	Number of deflectors
$N_{pasoscarc}$	Number of steps in the housing
$N_{pasostub}$	Number of steps in the tubes
N_{tubos}	Number of tubes
NTU	Number of heat transfer units
P_t	Distance between pipe centres
P_r	Prandtl number
Q_{total}	Total heat, W
Re_D	Reynolds Number
T_{ec}	Inlet temperature housing, $°C$
T_{sc}	Temperature of housing outlet $°C$
T_{et}	Tube inlet temperature, $°C$
T_{st}	Tube outlet temperature, $°C$
U	Overall Coefficient, $W/m^2 K$
u	Speed in the tubes, m/s
μ	Viscosity, $kg/m \cdot s$
ρ	Density, kg/m^3

REFERENCES

[1] "Asignatura, materias, Ingeniería Mecánica Barranquilla - Universidad del Norte." [Online]. Available: http://www.uninorte.edu.co/web/ingenieria-mecanica/plan-de-estudios. [Accessed: 19-Jul-2017].

[2] Universidad del Atlántico, "Ingeniería Mecánica | Universidad del Atlántico." [Online]. Available: https://www.uniatlantico.edu.co/uatlantico/docencia/ingenieria/programas/ingenieria-mecanica. [Accessed: 19-Jul-2017].

[3] T. S. Ge, W. Cao, X. Pan, Y. J. Dai, and R. Z. Wang, "Experimental investigation on performance of desiccant coated heat exchanger and sensible heat exchanger operating in series," Int. J. Refrig., 2017.

[4] S. V. A. Laakso, "Heat matters when matter heats – The effect of temperature-dependent material properties on metal cutting simulations," J. Manuf. Process., vol. 27, pp. 261–275, Jun. 2017.

[5] Y. Zhang, Y. Yang, Q. Li, and Y. Li, "Study on heat transfer model of coolant boundary layer during high speed cutting process," Int. J. Heat Mass Transf., vol. 114, pp. 1304–1313, 2017.

[6] M. L. Hosain, R. Bel Fdhila, and K. Rönnberg, "Taylor-Couette flow and transient heat transfer inside the annulus air-gap of rotating electrical machines," Appl. Energy, 2017.

[7] "VHP-T - KERN & SOHN GmbH." [Online]. Available: https://www.kern-sohn.com/shop/es/componentes/indicadores/VHP-T/. [Accessed: 19-Jul-2017].

[8] E. D. Técnico, "CONTROL ABIERTO + MULTICONTROL + CONTROL EN TIEMPO REAL."

[9] L. L. Cortés and E. M. Lango, "Simposio de Metrología EVALUACIÓN DE LA TRANSFERENCIA DE CALOR RADIAL POR EL ESPACIO ANULAR DE LA PLACA CALIENTE DE UN APARATO PARA MEDIR CONDUCTIVIDAD TÉRMICA."

[10] G. Rodríguez, "Sistema de Medición de la Conductividad Térmica de Materiales Sólidos Conductores , Diseño y Construcción," pp. 1–11, 2008.

[11] M. A. Ventura, "Conducción de calor radial en un elemento combustible de un reactor de potencia."

[12] W. Q. Li and Z. G. Qu, "Experimental study of effective thermal conductivity of stainless steel fiber felt," Appl. Therm. Eng., vol. 86, pp. 119–126, 2015.

[13] J. A. Ibáñez, F. J. Abellán, R. P. Valerdi, and J. A. García Gamuz, "Conductividad térmica de una barra de cobre. Estudio experimental del transitorio," Am. J. Phys. Educ, vol. 2, no. 3, 2008.

[14] Y. Z. Povstenko, "Fractional radial heat conduction in an infinite medium with a cylindrical cavity and associated thermal stresses," Mech. Res. Commun., vol. 37, no. 4, pp. 436–440, Jun. 2010.

[15] J. E. Doorly and M. L. G. Oldfield, "The theory of advanced multi-layer thin film heat transfer gauges," Int. J. Heat Mass Transf., vol. 30, no. 6, pp. 1159–1168, Jun. 1987.

[16] A. J. Schmidt, X. Chen, and G. Chen, "Pulse accumulation, radial heat conduction, and anisotropic thermal conductivity in pump-probe transient thermoreflectance," Rev. Sci. Instrum., vol. 79, no. 11, p. 114902, Nov. 2008.